Line-focus acoustic microscopy measurements of acoustic properties of LiTa03 crystal plates with an inversion layer

doi: 10.1063/1.365201

Line-focus acoustic microscopy measurements of acoustic properties of $LiTaO_3$ crystal plates with an inversion layer

Ailie Tourlog and Jan D. Achenbach[a)]
Center for Quality Engineering and Failure Prevention, Northwestern University, Evanston, Illinois 60208

J. Kushibiki
Department of Electrical Engineering, Tohoku University, Sendai 980, Japan

(Received 8 November 1996; accepted for publication 6 February 1997)

Inversion layers of 2 μm and 30 μm thickness were formed at the negative dipole-end $(-c)$ face of a Z-cut $LiTaO_3$ crystal plate by proton exchange followed by heat treatment. The phase velocities of leaky surface acoustic waves (LSAWs) on both the positive $(+c)$ and negative $(-c)$ faces of the plate were measured by line-focus acoustic microscopy versus the angle of propagation, at a frequency of 225 MHz, and the results were compared with theoretical predictions. It is shown that for an inversion layer of 30 μm thickness the phase velocities of LSAWs on the $+c$ and $-c$ faces are the same, and almost equal to the velocities of the virgin plate. This suggests that the material constants, which are decreased due to the proton exchange, are restored to the original values by the heat treatment. © *1997 American Institute of Physics.* [S0021-8979(97)03910-8]

I. INTRODUCTION

Domain inversion phenomena of $LiNbO_3$ and $LiTaO_3$ have been investigated in some detail in recent years.[1–5] In the inversion regions, the odd rank tensors, which represent piezoelectric, pyroelectric and nonlinear optic constants, change sign. This feature offers the possibility of applications of domain inversion in various fields, such as piezoelectric and surface acoustic wave devices,[6–8] optical second harmonic generation devices[9,10] and pyroelectric detectors.[11]

For $LiTaO_3$, the local ferroelectric domain inversion occurs at the $-c$ face of the plate when the plate is subjected to proton exchange and then heat treated at temperatures below the Curie point.[2,3] Proton exchange is known as a method for fabricating optical waveguides on $LiNbO_3$ and $LiTaO_3$ crystals.[12,13] The process results in a layer of a new crystalline structure, $H_xLi_{1-x}NbO_3$ or $H_xLi_{1-x}TaO_3$, with a large increase of extraordinary refractive index. It has been reported that the proton-exchange process leads to a large change of the velocity of surface acoustic waves (SAWs) on $LiNbO_3$ (Refs. 14–18) and $LiTaO_3$.[19] Specifically, it has been reported that the elastic constants of the proton-exchanged regions of $LiNbO_3$ are decreased[17,18] and the piezoelectric property is reduced to near zero in Y-cut $LiNbO_3$ (Ref. 15) and to 39% in 128°-rotated Y-cut $LiNbO_3$.[18] However it has also been reported that annealing restores the piezoelectric property and results in changes of the acoustic velocity,[14,15,18] but that saturation occurs after about 1 h of annealing time.[18] Tada *et al.*[20] have shown that for $LiTaO_3$ the variation of the refractive index changes to a Gaussian profile after annealing for 5 h at 400 °C, similar to that of proton-exchanged $LiNbO_3$.

In this article, a proton-exchanged $LiTaO_3$ plate is heated to a higher temperature, which gives rise to domain inversion on the $-c$ face of the plate. We investigate the related changes of the acoustic properties by the use of line-focus acoustic microscopy. It can be shown that there is no optical waveguide on the surfaces of the plate after the heat treatment at about 590 °C. Since the fabrication of the inversion domain of $LiTaO_3$ is based on the proton-exchange/heat treatment process, it is important to know the influence of this process on the acoustic properties of the inversion regions.

Line-focus acoustic microscopy (LFAM) is a useful technique to determine the elastic constants of bulk materials and thin films deposited on a substrate,[21–25] and to investigate the elastic properties of piezoelectric wafers.[26,27] The technique is based on the measurement of the $V(z)$ curve, which is the transducer output voltage V as a function of the distance between the focal line and the specimen surface. Both the phase velocity and the attenuation of a leaky surface acoustic wave (LSAW) can be determined from the periodic variation of the $V(z)$ curve. As reported in this article the phase velocities of the LSAWs of Z-cut $LiTaO_3$ plates with an inversion layer were measured by LFAM to investigate the acoustic properties of the inversion regions.

II. THEORETICAL CONSIDERATIONS

A. $V(z)$ measurement model

A $V(z)$ measurement model for nonpiezoelectric anisotropic-layer/anisotropic-substrate configurations for the line-focus acoustic microscope was described in Ref. 28. The model showed excellent agreement with experimental results.[28] According to the $V(z)$ measurement model, the output voltage of the transducer may be expressed as

$$V(z)=\int_{-\infty}^{+\infty} L_1(k_x)L_2(k_x)R(k_x)\exp(\mathrm{i}2k_z z)\,dk_x, \qquad (1)$$

where $k_z=\sqrt{k_w^2-k_x^2}$, and k_w is the wave number in the coupling fluid (water). Here $L_1(k_x)$ is the angular spectrum at the focal plane in water generated by an acoustic wave in the buffer rod, $L_2(k_x)$ is the voltage response of the transducer when a plane wave insonifies the lens, and $R(k_x)$ is the reflectance function of the fluid-specimen interface.

a)Electronic mail: achenbach@nwu.edu

 0021-8979/97/81(10)/6616/6/$10.00

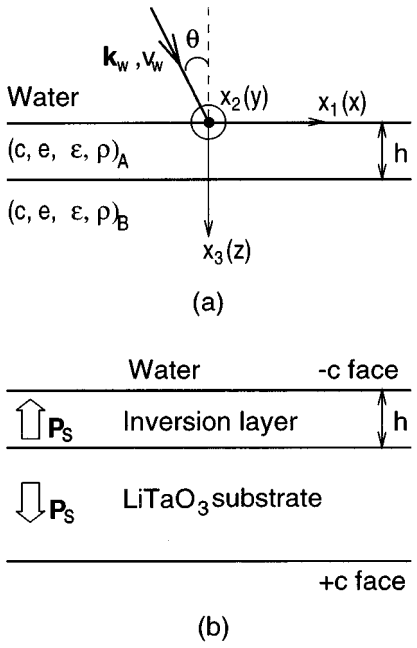

FIG. 1. (a) Incident wave and geometry of water-loaded single-layer/ substrate configuration. (b) Water-loaded $LiTaO_3$ substrate with an inversion layer (P_s: spontaneous polarization).

A detailed description and discussion of $L_1(k_x)$ and $L_2(k_x)$ can be found in Ref. 28, where integral expressions as well as numerical calculations were presented.

B. Reflectance function of layered piezoelectric solids

For fluid-loaded nonpiezoelectric anisotropic substrates and for fluid-loaded layered nonpiezoelectric anisotropic substrates, Nayfeh has proposed a numerical approach to calculate the reflectance function $R(k_x)$.[29] That approach is extended here to calculate the reflectance function for a water-loaded piezoelectric layer deposited on a piezoelectric substrate, as shown in Fig. 1(a). A plane wave with wave vector k_w and phase velocity v_w is incident on the specimen with an incident angle θ. The elastic constants c^E_{ijkl} $(i,j,k,l=1,2,3)$, piezoelectric constants e_{ijk}, and dielectric constants ε_{ij}, are transformed from the crystal coordinate system X, Y, Z to the x_1, x_2, x_3 (or x,y,z) coordinate system by a Euler transformation.[30]

In the piezoelectric medium the differential equation for displacements, u_i, and the electric potential, φ, are given as follows[31]

$$c^E_{ijkl}u_{k,li}+e_{kij}\varphi_{,ki}=\rho\ddot{u}_j, \tag{2}$$

$$e_{ikl}u_{k,li}-\varepsilon^S_{ik}\varphi_{,ki}=0. \tag{3}$$

The piezoelectric constitutive equations are

$$T_{ij}=c^E_{ijkl}S_{kl}-e_{kij}E_k, \tag{4}$$

$$D_i=e_{ikl}S_{kl}+\varepsilon^S_{ij}E_k, \tag{5}$$

and

$$S_{i,j}=\tfrac{1}{2}(u_{i,j}+u_{j,i}), \tag{6}$$

$$E_i=-\varphi_{,i}, \tag{7}$$

where T_{ij} are the stress components, D_i the electric displacements, S_{ij} the strain components and E_i the electric field components in the quasielectrostatic approximation. The general solutions of Eqs. (2) and (3) are

$$u_i=\sum_{n=1}^{8} A_n\beta_{in}\exp[i\xi(x_1+\alpha_n x_3-vt)], \tag{8}$$

$$\varphi=\sum_{n=1}^{8} A_n\beta_{4n}\exp[i\xi(x_1+\alpha_n x_3-vt)], \tag{9}$$

where $\xi=k_w\sin\theta$, $v=v_w/\sin\theta$, and $\xi\alpha_n$ is the wave number in direction x_3, β_{in} are constants associated with α_n, and A_n are unknown coefficients that will be determined by boundary conditions. Upon substitution of Eqs. (8) and (9) into Eqs. (4)–(7), the displacements, the stress components on a surface normal to x_3, the electric potential and the normal electric displacement in the layer may be written as

$$\begin{bmatrix} u_1\\ u_2\\ u_3\\ \varphi\\ T_{33}\\ T_{13}\\ T_{23}\\ D_3 \end{bmatrix} = [M^L(x_3)] \begin{bmatrix} A_1\\ A_2\\ A_3\\ A_4\\ A_5\\ A_6\\ A_7\\ A_8 \end{bmatrix}. \tag{10}$$

Beginning with Eq. (10), the term $\exp[i\xi(x_1-vt)]$ was omitted. In the substrate, using the same procedure, the corresponding relations are

$$\begin{bmatrix} u_1\\ u_2\\ u_3\\ \varphi\\ T_{33}\\ T_{13}\\ T_{23}\\ D_3 \end{bmatrix} = [M^S(x_3)] \begin{bmatrix} B_1\\ B_2\\ B_3\\ B_4\\ 0\\ 0\\ 0\\ 0 \end{bmatrix}. \tag{11}$$

Here $[M^L(x_3)]$ and $[M^S(x_3)]$ are 8×8 matrices that can easily be derived from Eqs. (4)–(9), but they are not listed here for brevity. The coefficients B_n $(n=5,6,7,8)$ are set equal to zero in order to satisfy the outgoing wave condition. The terms in column vectors on the left-hand sides of Eqs. (10) and (11) do not all have the same physical dimension. The dimensions of the corresponding terms in the matrices $[M^L(x_3)]$ and $[M^S(x_3)]$ are, however, such that the actual equations corresponding to Eqs. (10) and (11) have the proper dimensions on both sides of the equality signs. It might be added that in the numerical work all quantities are made dimensionless.

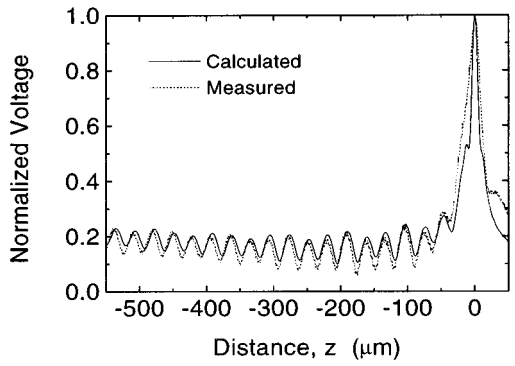

FIG. 2. Comparison of calculated and measured $V(z)$ curves for virgin ZX $LiTaO_3$ ($f=225$ MHz).

At the interface between the layer and the substrate, $x_3=h$, the displacements u_i, stress components T_{i3}, electric potential φ and electric displacement D_3 are continuous, that is,

$$[M^{\mathrm{L}}(h)]\begin{bmatrix} A_1 \\ A_2 \\ A_3 \\ A_4 \\ A_5 \\ A_6 \\ A_7 \\ A_8 \end{bmatrix} = [M^{\mathrm{S}}(h)]\begin{bmatrix} B_1 \\ B_2 \\ B_3 \\ B_4 \\ 0 \\ 0 \\ 0 \\ 0 \end{bmatrix}. \tag{12}$$

It follows that at $x_3=0$ the displacements, the stress components, the electric potential and the electric displacement may be written as

$$\begin{bmatrix} u_1 \\ u_2 \\ u_3 \\ \varphi \\ T_{33} \\ T_{13} \\ T_{23} \\ D_3 \end{bmatrix}_{x_3=0} = [N]\begin{bmatrix} B_1 \\ B_2 \\ B_3 \\ B_4 \\ 0 \\ 0 \\ 0 \\ 0 \end{bmatrix}, \tag{13}$$

where

$$[N]=[M^{\mathrm{L}}(0)][M^{\mathrm{L}}(h)]^{-1}[M^{\mathrm{S}}(h)]. \tag{14}$$

For an incident and reflected wave in water, the normal displacement and the normal stress at $x_3=0$ are

$$\begin{bmatrix} u_3 \\ T_{33} \end{bmatrix}_{x_3=0} = \begin{bmatrix} \cos\theta \\ \mathrm{i} \end{bmatrix} + \begin{bmatrix} -\cos\theta \\ \mathrm{i} \end{bmatrix} R, \tag{15}$$

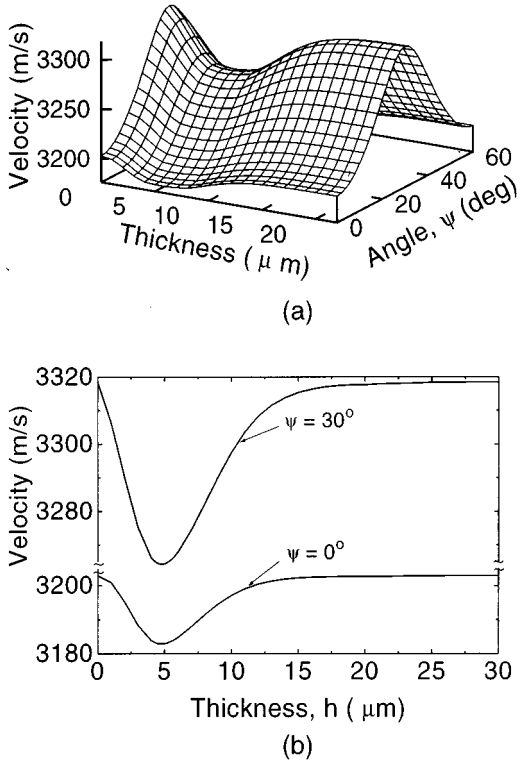

FIG. 3. (a) Calculated phase velocities of LSAWs on Z-cut $LiTaO_3$ as a function of propagation angle from X axis, ψ, and thickness of the inversion layer, h. (b) Variation of the phase velocity with inversion layer thickness at $\psi=0°$ and $\psi=30°$ ($f=225$ MHz).

where R is the reflection coefficient. Neglecting the conductivity of water, the normal electric displacement D_3 at $x_3=0$ may be expressed by

$$D_3|_{x_3=0} = -\varepsilon_{\mathrm{w}}\xi[N_{41}N_{42}N_{43}N_{44}]\begin{bmatrix} B_1 \\ B_2 \\ B_3 \\ B_4 \end{bmatrix}, \tag{16}$$

where ε_{w} is the dielectric constant of water.

At the interface between water and the layer ($x_3=0$) u_3, T_{i3}, and D_3 must be continuous, which leads to the following set of equations using Eqs. (13), (15), and (16):

$$\begin{bmatrix} \cos\theta \\ \mathrm{i} \\ 0 \\ 0 \\ 0 \end{bmatrix} = \begin{bmatrix} N_{31} & N_{32} & N_{33} & N_{34} & \cos\theta \\ N_{51} & N_{52} & N_{53} & N_{54} & -\mathrm{i} \\ N_{61} & N_{62} & N_{63} & N_{64} & 0 \\ N_{71} & N_{72} & N_{73} & N_{74} & 0 \\ N'_{81} & N'_{82} & N'_{83} & N'_{84} & 0 \end{bmatrix}\begin{bmatrix} B_1 \\ B_2 \\ B_3 \\ B_4 \\ R \end{bmatrix}, \tag{17}$$

where $N'_{8n}=N_{8n}+\varepsilon_{\mathrm{w}}\xi N_{4n}$ $(n=1,2,3,4)$. The reflection coefficient R, which is the reflectance function $R(k_x)$ for $k_x\equiv\xi=k_{\mathrm{w}}\sin\theta$, is then obtained by solving Eq. (17).

TABLE I. Phase velocities of the Z-cut $LiTaO_3$ plates. (PE: proton exchange, heat: heat treatment.)

Process	Method	Angle ψ (deg)	Velocity $+c$ (m/s)	Velocity $-c$ (m/s)
Virgin	calculated	0	3202.90	3202.90
(unprocessed)		30	3318.46	3318.46
	measured	0	3199.0±0.4	3199.0±0.4
	(average)	30	3309.9±0.5	3309.9±0.5
PE	measured	0	3125.41	3138.23
		30	3209.23	3232.13
PE+heat	measured	0	3197.30	3196.86
$h\approx 30$ μm	(# 1)	30	3307.33	3306.82
	measured	0	3197.44	3197.89
	(# 2)	30	3307.36	3307.46
	measured	0	3197.01	3196.53
	(# 3)	30	3306.66	3306.44
	measured	0	3195.86	3195.42
	(# 4)	30	3306.28	3305.84
	measured	0	3197.01	3196.59
	(# 5)	30	3307.36	3306.92
	average	0	3196.9±0.4	3196.7±0.5
		30	3307.0±0.4	3307.0±0.4
PE+heat	measured	0	3194.04	3191.95
$h\approx 2$ μm		30	3300.44	3285.08
	calculated	0	3202.90	3195.18
		30	3318.46	3290.01
Heat only	measured	0	3197.09	3196.98
		30	3307.42	3307.37

C. *V(z)* curve of *Z*-cut $LiTaO_3$

Next, let us consider a Z-cut $LiTaO_3$ crystal with an inversion layer of thickness h at the $-c$ face, as shown in Fig. 1(b). If there is no influence of the proton-exchange and heat treatment processes on the material constants of the inversion regions, then the elastic constants of the inversion regions are identical to those of the original crystal, and the piezoelectric constants are opposite in sign.

The $V(z)$ curve for a virgin ZX $LiTaO_3$ plate calculated by Eq. (1) is shown in Fig. 2 by the solid line. Material constants used in this numerical calculation were taken from the work of Warner *et al.*[32]

III. EXPERIMENTAL WORK

A Honda AMS-5000 ultrasonic measurement system with a line-focus acoustic lens operating at 225 MHz was used to measure the velocities. Two-in.-diam and 0.5-mm-thick optical-grade single-domain Z-cut $LiTaO_3$ crystal wafers polished on both faces were used in the experiments. Eight 6 mm×7 mm rectangular specimens were sectioned from the centers of the wafers. The velocity of the LSAW was measured at the center of the specimens. The curie temperature of the wafers is about 604 °C.

For virgin $LiTaO_3$ the measured $V(z)$ curve in the X direction ($\psi=0°$) is shown in Fig. 2 by the dashed line for comparison with the calculated curve.

Proton exchange in the plates was carried out in a melt of benzoic acid for 6 h at 220 °C. The subsequent heat treatment was carried out in air. To get the desired thickness of the inversion layer, the temperature and time both for rising to the treatment temperature and for treatment were varied; see Refs. 2, 3, and 33. In this study, specimens with an inversion layer of about 30 μm and 2 μm were used. It can be shown using a rutile prism coupler that the optical waveguides disappear on both surfaces after the heat treatment, which indicates that there is no longer a higher extraordinary refractive index layer on the surfaces of the plates.

IV. RESULTS AND DISCUSSION

A. Theoretical phase velocities

By $V(z)$ curve analysis, the velocity of LSAWs can be calculated from[21]

$$v=\frac{v_w}{\sqrt{1-[1-(v_w/2f\Delta z)]^2}}, \tag{18}$$

where v_w is the wave velocity in water ($v_w=1490$ m/s), f is the operating frequency, and Δz is the periodic dip interval of the $V(z)$ curve.

The phase velocities of LSAWs on a Z-cut $LiTaO_3$ plate with an inversion layer were calculated using the $V(z)$ measurement model. Figure 3 shows the phase velocities of LSAWs on Z-cut $LiTaO_3$ as a function of the angle, ψ, from the X axis, and the thickness of the inversion layer, h. The calculation was carried out at a frequency of 225 MHz. For thin layers dispersion of the LSAWs occurs due to an electric-field short-circuiting effect on the interface of the layer and the substrate.[34] Similar results were also found in Y-cut $LiTaO_3$ and $LiNbO_3$ substrates in air.[35,36] For $\psi=0°$ and $\psi=90°$ (or 30°) the velocity as a function of h is shown in Fig. 3(b). The velocities decrease with increasing h. When the inversion layer is thick enough, $h>25$ μm, the velocities return to those of LSAWs on virgin plates. Thus, the velocities on the $-c$ face are identical to those on the $+c$ face when the inversion layer is thicker than 25 μm.

B. Measured phase velocities

The accuracy of the experimental procedure was established as 0.005%; see, for example, Refs. 26 and 27. For wave speeds of the order of 3200 m/s, this corresponds to 0.16 m/s. In addition there are variations due to the inhomogeneity of the material,[26,27] and hence the eight specimens produce slightly different wave speeds. For the virgin wafer Table I lists the average phase velocity for the eight specimens together with the maximum deviations. Thus these maximum deviations include both the measurement error and the effect of inhomogeneity.

The differences between the velocities of the $+c$ and $-c$ faces are within ± 0.5 m/s.

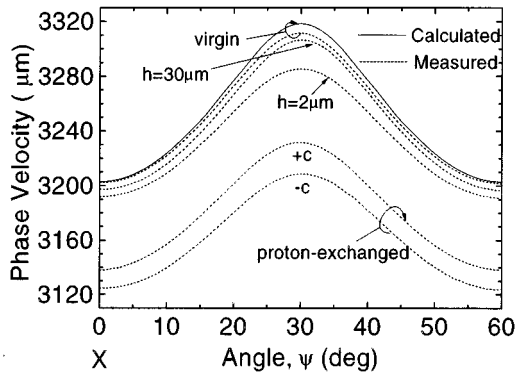

FIG. 4. Comparison of the measured and calculated directional variations of the phase velocities for the Z-cut $LiTaO_3$ plates ($f=225$ MHz).

Figure 4 shows the variation of measured velocities with angle ψ for one of the specimens compared to the calculated results. Both calculated and measured velocities for $\psi=0°$ and $\psi=30°$ are also listed in Table I. The measured velocities of the virgin specimens are a little lower than the calculated ones especially at $\psi=30°$. As compared to the virgin material, the velocities in the proton-exchanged regions of the $-c$ face are reduced by about 2% and 3% at $\psi=0°$ and $\psi=30°$, respectively; see the row labeled PE in Table I. Because of nonuniform heating on both sides of the plate during the proton exchange, the thickness of the proton-exchanged layers may be different. Consequently, the velocities at both sides are different.

For the specimens with an inversion layer of about 30 μm, which were heat treated for 3 h at about 587 °C, the velocities of the $+c$ and $-c$ faces are also listed in Table I. The numbers in Table I represent five specimens. The differences between the velocities of the $+c$ and $-c$ faces are about ± 0.5 m/s. This shows that the material constants are almost the same on both faces of the plate. The average phase velocities for the five specimens are also listed together with the maximum deviations. The velocities are a little lower (0.06% and 0.09%) than the velocities of the virgin plate. It is likely that out-diffusion of Li_2O occurs during the heat treatment. In order to confirm this, a virgin specimen was heat treated under the same conditions but without proton exchange. The measured velocities at both the $-c$ and $+c$ faces of this plate are equal to those of the plates with an inversion layer of 30 μm and those results are also listed in Table I. To prevent out-diffusion of Li_2O, water vapor should be added to the atmosphere of the gases.

The measured velocities of the specimen with an inversion layer of 2 μm are also listed in Table I, but only the measured and calculated velocities at the $-c$ face are shown in Fig. 4. The plate was heat treated for 5 h to reach 590 °C and then was kept for 1 h at 590 °C. Since there is a thin inversion layer of 2 μm on the $-c$ face, the velocities at the $-c$ face are lower than those at the $+c$ face. The velocities at the $+c$ face are a little lower than those on the plate with an inversion layer of 30 μm because of the longer heat treatment. The errors for these latter results are just the measurement errors of 0.005%.

V. CONCLUSION

The $V(z)$ measurement model has been extended to a thin piezoelectric layer on a piezoelectric substrate. The phase velocities of Z-cut $LiTaO_3$ plates with an inversion layer were calculated by the model. The velocities of LSAWs on both the $+c$ and $-c$ faces of Z-cut $LiTaO_3$ plates, where the latter has an inversion layer, were measured by LFAM. The measured velocities of the plate, with a thin layer of 2 μm, show differences between the velocities on the $+c$ face and $-c$ face, that confirm the theoretical values. For a thickness of the inversion layer of 30 μm, the velocities on both faces are the same, in agreement with the calculated values. The latter results suggest that the material constants of the inversion layers formed by proton exchange followed by heat treatment have not changed significantly from those of the virgin material, and that the elastic and piezoelectric constants that are reduced due to proton exchange are restored by the heat treatment.

ACKNOWLEDGMENTS

The authors are pleased to acknowledge helpful discussions with Professor K. Nakamura of Tohoku University. This work was carried out in the course of research sponsored by the Office of Naval Research under Contract No. N00014-89-J-1362.

[1] K. Nakamura, H. Ando, and H. Shimizu, Appl. Phys. Lett. **50**, 1413 (1987).
[2] K. Nakamura and H. Shimizu, Appl. Phys. Lett. **56**, 1535 (1990).
[3] K. Nakamura, M. Hosoya, and A. Tourlog, J. Appl. Phys. **73**, 1390 (1993).
[4] K. Nakamura and A. Tourlog, Appl. Phys. Lett. **63**, 2065 (1993).
[5] A. Tourlog and K. Nakamura, Jpn. J. Appl. Phys. 1 **32**, 4370 (1993).
[6] K. Nakamura, H. Ando, and H. Shimizu, Proceedings of the IEEE Ultrasonics Symposium, 1986 (IEEE, New York, 1986), p. 719.
[7] K. Nakamura, Jpn. J. Appl. Phys. 1 **31**, 9 (1992).
[8] K. Nakamura and A. Tourlog, IEEE Trans. Ultrason. Ferroelectr. Freq. Control **41**, 872 (1994).
[9] J. Webjörn, F. Laurell, and G. Arvidsson, J. Lightwave Technol. **7**, 1597 (1989).
[10] K. Mizuuchi, K. Yamamoto, and T. Taniuchi, Appl. Phys. Lett. **58**, 2732 (1991).
[11] K. Nakamura and M. Itagaki, Jpn. J. Appl. Phys. 1 **33**, 5404 (1994).
[12] J. L. Jackel, C. E. Rice, and J. J. Veselka, Appl. Phys. Lett. **41**, 607 (1982).
[13] W. B. Spillman, Jr., N. A. Sanford, and R. A. Soref, Opt. Lett. **8**, 497 (1983).
[14] V. Hincov, J. Appl. Phys. **62**, 3573 (1987).
[15] F. S. Hickernell, K. D. Ruehle, S. J. Joseph, G. M. Reese, and J. F. Weller, Proceedings of the IEEE Ultrasonics Symposium, 1985 (IEEE, New York, 1985), p. 237.
[16] P. J. Burnett, G. A. D. Briggs, S. M. Al-Shukri, J. F. Duffy, and R. M. De La Rue, J. Appl. Phys. **60**, 2517 (1986).
[17] E. M. Bieble, P. H. Russer, and K. Anemogianns, Proceedings of the IEEE Ultrasonics Symposium, 1989 (IEEE, New York, 1989), p. 281.
[18] S. Kakio, J. Matsuoka, and Y. Nakagawa, Jpn. J. Appl. Phys. 1 **32**, 2359 (1993).
[19] M. Hirabayashi, T. Yamasaki, and Y. Komatsu, Jpn. J. Appl. Phys. 1 **32**, 2355 (1993).
[20] K. Tada, T. Murai, T. Nakabayashi, T. Iwashima, and T. Ishikawa, Jpn. J. Appl. Phys. 1 **26**, 503 (1987).
[21] J. Kushibiki and N. Chubachi, IEEE Trans. Sonics Ultrason. **SU-32**, 189 (1985).
[22] J. Kushibiki, J. Acoust. Soc. Jpn. **45**, 294 (1989) (in Japanese).

[23] J. D. Achenbach, J. O. Kim, and Y.-C. Lee, *Advances in Acoustic Microscopy*, edited by A. Briggs (Plenum, New York, 1995), Vol. I, Chap. 5.
[24] Y.-C. Lee, J. O. Kim, and J. D. Achenbach, IEEE Trans. Ultrason. Ferroelectr. Freq. Control **42**, 253 (1995).
[25] Y.-C. Lee, J. D. Achenbach, M. J. Nystrom, S. R. Gilbert, B. A. Block, and B. W. Wessels, IEEE Trans. Ultrason. Ferroelectr. Freq. Control **42**, 376 (1995).
[26] J. Kushibiki, H. Takahashi, T. Kobayashi, and N. Chubachi, Appl. Phys. Lett. **58**, 893 (1991).
[27] J. Kushibiki, H. Ishiji, T. Kobayashi, N. Chubachi, I. Sahashi, and T. Sasamata, IEEE Trans. Ultrason. Ferroelectr. Freq. Control **42**, 83 (1995).
[28] Y. -C. Lee, J. O. Kim, and J. D. Achenbach, J. Acoust. Soc. Am. **94**, 923 (1993).
[29] A. H. Nayfeh, Wave Motion **14**, 55 (1991).
[30] L. M. Brekovskikh, *Waves in Layered Media* (Academic, New York, 1960), Chap. 1.
[31] B. A. Auld, *Acoustic Fields and Waves in Solids* (Wiley, New York, 1973).
[32] A. W. Warner, M. Onoe, and G. A. Coquin, J. Acoust. Soc. Am. **42**, 1223 (1967).
[33] A. Tourlog and K. Nakamura, Proceedings of the IEEE 9th International Symposium on Applications of Ferroelectrics, 1994, p. 222.
[34] K. Nakamura, A. Tourlog, and H. Shimizu, Proc. Acoust. Soc. Jpn. **2**, 695 (1988) (in Japanese).
[35] A. Tourlog, K. Nakamura, and H. Shimizu, Tech. Rep. IEICE **US89-44**, 47 (1994) (in Japanese).
[36] K. Nakamura and A. Tourlog, Jpn. J. Appl. Phys. 1 **34**, 5273 (1995).